Available online at: http://www.ijmtst.com/vol5issue12.html

International Journal for Modern Trends in Science and Technology

ISSN: 2455-3778 :: Volume: 05, Issue No: 12, December 2019

# 3-D Simulation of Turbulent Dispersion in Evaporating Sprays

Aryan YousefyanKelareh[1] | Pouria Karimi Shahri [2]

[1]Mechanical Engineering Department, TarbiatModares University, Tehran, Iran

[2]Mechanical Engineering Department, University of North Carolina at Charlotte, North Carolina, USA

**To Cite this Article**

Aryan YousefyanKelareh and Pouria Karimi Shahri, "3-D Simulation of Turbulent Dispersion in Evaporating Sprays", *International Journal for Modern Trends in Science and Technology*, Vol. 05, Issue 12, December 2019, pp.-01-08.

**Article Info**

Received on 09-November-2019, Revised on 18-November-2019, Accepted on 27-November-2019, Published on 30-November-2019.

## ABSTRACT

*The present study investigates the results of an in-house three-dimensional CFD code, which is designed for diesel engine spray calculations. Besides, the importance of implementing different turbulent dispersion models is studied. The effects of gas-phase turbulence on the final spray structure and the fuel droplet trajectory are considered by utilizing various turbulent dispersion models. Finally, the implementation of the droplet dispersion models was compared to that of the droplet trajectory and other information. Furthermore, the importance of choosing a proper turbulence closure model is addressed.*

**KEYWORDS:** *Turbulent dispersion; Turbulence modulation; Diesel engine; Two-way coupling.*

*Copyright © 2019 International Journal for Modern Trends in Science and Technology*
*All rights reserved.*

## I. INTRODUCTION

The emission of diesel engines has drastically cut the attention of many researchers to enhance their efficiency. To reach an efficient combustion process, the quality of fuel-air mixture formation should be taken into account as an active parameter. To provide a better understanding of in-cylinder flows, one can develop CFD codes as a practical approach. These 3D analyses extensively describe combustion chamber turbulent flows formed. Once fuel droplets are added to this turbulent flow, the problem becomes more substantially complicated, i.e. lack of insight into the elemental physics of the droplet-gas flow interaction. Therefore, the applied models crucially need to be accurate in these calculations. Droplets do not thoroughly travel within the carrier phase path in turbulent spray flows, but rather the interaction between droplets and fluctuating velocity yields their rapid dispersion. Implementing dispersion models to evaluate RMS values (once employing RANS equations), the instantaneous fluid velocity is obtained on the site of a droplet. Using irrelevant dispersion/turbulence models, there is the possibility to reach nonphysical results [1-3].

A stochastic model was proposed by Yuu and Yasukouchi, Hirosawa [4], which addresses the empirical correlation of mean and turbulent properties. This model was then modified by Gosman and Ioannides [5] to cover the eddy-particle relative velocity. The modified model was entitled "eddy lifetime model," in which fluid velocity has invariant fluctuation on the Lagrangian time scale [6] for the sake of simplicity, making the model commonly used in the majority of commercial CFD codes. However, this model fails to be viable in anisotropic turbulent flows since it excludes spatial and time correlation of the

fluctuation across the particle path [7]. In this regard, Fluctuation velocity was rebuilt out of a time-correlated random-walk model by Hunt and Nalpanis [8] to address time correlation. This model takes advantage of the crossing trajectory effect, the Lagrangian flow time-scale from the particle perspective". Furthermore, the Sommerfeld model [9-11] can incorporate both spatial and time correlations, which was derived from a Markov-chain random-walk model. In this model, fluctuation velocities along the streamline and at the droplet location are assessed by a Lagrangian correlation factor (time correlation) and a Eulerian correlation factor (spatial correlation), respectively. The primary purpose of the existing research is to investigate droplet dispersion and evaporation of diesel engine fuel spray as critical factors in the prediction of the effectiveness of spray ignition-equipped energy systems.

## II. GOVERNING EQUATIONS

This section extensively describes the models applied to the in-house CFD code to solve the fuel-droplet spray injection in the combustion chamber of a diesel engine. To solve the two-phase flow, the Eulerian-Lagrangian approach was implemented wherein the dispersed phase (fuel droplets) and the continuous phase (air-fuel vapor mixture) were treated by Eulerian and Lagrangian equations, respectively. A limited number of parcels were employed to describe the spray, exhibiting droplets with the same diameter, velocity, temperature, and location. In what follows, the governing equations of both phases and their interactions are explained in complete detail.

### A. Gas-phase equations

This section introduces the governing equations of gas phase needed to perform a thorough analysis of the problem. Regarding the continuous phase, eight partially-differential equations were solved, namely conservation of mass, momentum (in three directions), turbulent kinetic energy, turbulent dissipation rate, energy, and fuel vapor mass fraction are solved. As already mentioned, the RANS models were implemented to treat the turbulent flow. The turbulent flow was solved using RANS models and the Standard $k-\varepsilon$ and $RNGk-\varepsilon$ models were chosen and compared with each other [12]. In addition, we can use the equations in ensemble-averaged, if assumed that their statistically averaged characteristics can describe the in-cylinder processes [13]. In the present study, the used averaging method is density-weighted or Favre averaging.

Since the piston moves with a local absolute value ($u_{grid}$), the volume of computational cells would face a variation needed to be incorporated into the equations. Thus, the general transport equation is written as follows:

$$\frac{1}{\delta V}\frac{\partial(\rho\delta V\phi\theta)}{\partial t}+\nabla.(\rho\phi u_{rel}\theta) = \nabla.(\theta\Gamma_{\phi}\nabla.\phi)+S_{\phi}+S_{\phi,d} \quad (1)$$

where, $u_{rel}=u-u_{grid}$ stands for the frame-fluid relative velocity, $\delta V=\Delta x\Delta y\Delta z$ denotes the volume of a computational cell. In addition, the void fraction of a cell is represented by $\theta$ where a portion of which is filled with the gas mixture, $\rho$ is the mixture density, $\phi$ is the transported variable, $S_{\phi}$ is the source term, and $S_{\phi,d}$ is the source term due to the interactions of the droplet phase. The definitions of $\phi$, $\Gamma$, and $S$ are listed in Table I. By the addition of source terms to appropriate equations, the particles-gas phase interactions were concerned.

### B. Droplet equations

The second phase equations are written in the Lagrangian frame which is natural for tracking droplets.

The droplet momentum and trajectory equations adopted in this work are as follows:

$$K_d=\frac{3}{4}C_d(\frac{\rho_g}{\rho_d})\frac{1}{D_d}|u_i-u_{i,d}|\frac{du_{i,d}}{dt} = K_d(u_i-u_{i,d})-\frac{1}{\rho_d}\left(\frac{dp}{dx_i}\right) \quad (2)$$

$$\frac{dx_{i,d}}{dt}=u_{i,d} \quad (3)$$

Table I. Transport equation variables

| Variable | $\phi$ | $\Gamma_{\phi}$ | $S_{\phi}$ |
|---|---|---|---|
| Mass | 1 | 0 | 0 |
| Velocity | $u$ | $\mu_{eff}$ | $\theta\ \partial p/(\partial x_i)$ |
| Energy | $h$ | $\frac{\mu_{eff}}{\sigma_h}$ | 0 |
| Turbulent kinetic energy | $k$ | $\frac{\mu_{eff}}{\sigma_k}$ | $P_k-\varepsilon$ |
| Eddy dissipation rate | $\varepsilon$ | $\frac{\mu_{eff}}{\sigma_{\varepsilon}}$ | $C_{1\varepsilon}(\varepsilon/k)(P_k)-C_{2\varepsilon}(\varepsilon^2/k)$ |
| Fuel vapor mass fraction | $f$ | $D$ | 0 |

The Reynolds number is used to evaluate the drag coefficient$C_d$, thus:

$$C_d = \begin{cases} 0.44 & Re_d > 1000 \\ (24 + 3.6Re_d^{0.687})/Re_d & Re_d \leq 1000 \end{cases} \quad (4)$$

where particle Reynolds number is defined as: $Re_d = \rho_g|u_g - u_d|D_d/\mu_g$. In (5) two important forces considered in this work are drag and pressure difference forces. In (6), $x_{i,d}$ represents the spatial coordinate and $t$ represents temporal coordinate, and $u_{i,d}$ is droplet velocity. Also, $\rho_g$ and $\rho_d$ are the gas and droplet density respectively, $p$ is the pressure, $C_d$ is the drag coefficient, and $D_d$ is the droplet diameter. In (5), we should calculate the relative velocity between the gas phase and droplet$(u_i - u_{i,d})$. Because of using RANS equations for solving the turbulent flow, just the averaged velocities are obtained. Because the main focus of this work is on dispersion models, details of the three models adopted for comparison will be discussed in a separate section. Droplet temperature and mass histories are calculated from equations of Borman and Johnson [14] equations:

$$\frac{d(mC_pT)_d}{dt} = -\pi D_d K\left(T_g - T_d\right)\{z/(e^z - 1)\}Nu + Q\frac{dm_d}{dt} \quad (5)$$

$$\frac{dm_d}{dt} = -\pi D_d D P_t \ln\{(P_t - P_{v,\infty})/(P_t - P_{v,s})\}Sh/RT_m \quad (6)$$

where $D$ is the diffusivity, $P_t$ is the total pressure, $P_{v,\infty}$ is the vapor pressure far from the droplet surface, $P_{v,s}$ is the vapor pressure at the droplet surface, $R$ is the global gas constant, $T$ is the temperature, the subscripts $m$ denotes a mean of gas and droplet values, $C_p$ is the specific heat at constant pressure, $K$ is the thermal conductivity and $Q$ is the latent heat of evaporation. $z$ in (5) is the argument of a function which corrects the heat transfer coefficient when the mass transfer is simultaneously taking place, and is defined as:

$$z = -\frac{C_{pv}\frac{dm_d}{dt}}{\pi D_d KNu} \quad (7)$$

where $C_{pv}$ is the fuel vapor specific heat. The Nusselt number, $Nu$ and Sherwood $Sh$ are evaluated from the following expressions [15]:

$$Nu = 2.0 + 0.6\,Re_d^{0.5}Pr^{1/3} \quad (8)$$

$$Sh = 2.0 + 0.6\,Re_d^{0.5}Sc^{1/3} \quad (9)$$

where $Sc = \frac{\mu_g}{\rho_g D}$ , $= \frac{C_{pg}\mu_g}{K}$ , and $\mu_g$ is the gas viscosity. In this work, a fully atomized model has been used and the initial droplets diameters are calculated based on Rosin-Rammler probability density function. Two active forces on droplets are aerodynamic forces and forces due to surface tension. The condition, which the droplet goes under certain deformation, is when the aerodynamic forces overcome surface tension forces. One of the models which is very famous for modeling breakup process is Ritz-Diwakar model [16]. This model considers two modes of breakup: Bag breakup for low Weber numbers and stripping breakup for higher Weber numbers. The threshold for the start of breakup is $We_c = 6$ which this model decides which mode of the breakup will happen for the parcel of droplets.

### C. *Turbulent dispersion models*

Taking advantage of simplicity while the accuracy of RANS equations provides us with time-averaged velocities of the flow field. But for calculating the trajectory of droplets as accurate as possible, we should incorporate appropriate models for attaining velocity fluctuations at the droplet location. In this work, three models have been chosen to assess their capability of predicting the fuel droplet trajectory, accurately. The first and most known model is the model of Gosman and Ionnadies [5] which considers a constant fluctuation velocity in the integration time scale period. This model generates a random number from a normal distribution, which has a zero mean and a unit standard deviation (Γ) and multiplies it in the square root of gas flow's turbulent kinetic energy:

$$u' = \Gamma\sqrt{\frac{2k}{3}} \quad (10)$$

Here $u'$ is the fluctuation velocity, which will be added to a time averaged velocity, Γ is a random number and $k$ is the turbulent kinetic energy of gas mixture in droplet cell. The second model used in this work is Hunt and Nalpanis [8] model which calculates the fluctuation velocity from a temporally correlated random-walk model as:

$$u'(t + \Delta t) = u'(t)R_T(\Delta t) + \sqrt{1 - R_T^2(\Delta t)}\left(\Gamma(t)\sqrt{\frac{2k(t)}{3}}\right) \quad (11)$$

where the auto-correlation function is defined as:

$$R_T(\Delta t) = \exp\left(-\frac{\Delta t}{T_L}\right) \quad (12)$$

and $T_L$ is the Lagrangian time-scale of the continuous phase seen by the particle, which is related to the turbulence time-scale of the gas phase ($T_L^{(f)}$) by

$$T_L = T_L^{(f)}\left[1+\left(\frac{|u-u_d|}{\sqrt{\frac{2k(t)}{3}}}\right)^{\frac{2}{3}}\right]^{-1} \quad \text{and} \quad T_L^{(f)} = C_\mu^{3/4}\frac{k}{\varepsilon\sqrt{2/3}} \quad (13)$$

This autocorrelation function produces a new fluctuation velocity based on the previous time step fluctuation velocity and takes into account the temporal variation of it by $R_T(\Delta t)$.The third model is the Sommerfeld [11] model which uses both temporal and spatial correlations to produce the fluctuation velocity in this time step as:

$$u_i'(t+\Delta t) = u_i'(t)R_{P_i}(\Delta t, \Delta r) + \Gamma_i(t)\sqrt{1-R_{P_i}^2(\Delta t,\Delta r)}\sqrt{\frac{2k(t)}{3}} \quad (14)$$

The solution of (14) for an initial condition represents a sequence of successive velocities. In this equation, $\Delta r$ represents the spatial displacements during the $\Delta t$ interval and $R_P(\Delta t, \Delta r)$ is a correlation for computing the fluctuation velocity:

$$R_{P_i}(\Delta t, \Delta r) = R_{L_i}(\Delta t) * R_{E_i}(\Delta r) \quad (15)$$

The evolution of the fluid velocity along the path is declared by the Lagrangian correlation factor$R_{L_i}(\Delta t)$, while the fluid velocity is correlated with the fluid element location by using the Eulerian correlation factor $R_{E_i}(\Delta r)$ . They are expressed as:

$$R_{L_i}(\Delta t) = \exp\left(-\frac{\Delta t}{T_{L_i}}\right) \quad (16)$$

$$R_{E_i}(\Delta r) = \left(\exp\left(-\frac{\Delta r}{L_E}\right) - \left(1-\frac{\Delta r}{2L_E}\right)\exp\left(-\frac{\Delta r}{L_E}\right)\right)\frac{\Delta r_i \Delta r_j}{\Delta r^2} + (\Delta r)\left(1-\frac{\Delta r}{2L_E}\right)\exp\left(-\frac{\Delta r}{L_E}\right)\delta_{ij} \quad (17)$$

$T_{L_i}$ represents the Lagrangian integral time scale which is calculated as $T_{L_i} = 0.3\,k/\varepsilon$ and $L_E = 0.3T_L\sqrt{k}$ represents the turbulent length scale.

## III. Validation and Results

This section begins with presenting the mesh independency results. Next section will be on the single parcel injection in a quiescent flow (constant volume) and the final section will represent the effect of using different dispersion models in a full spray structure.

### A. Grid Independence results

Three different computational meshes which have a different number of cells are chosen to assess the grid independent results. Both the single-phase and two-phase characteristics are compared to reach grid independent results. For single phase mesh independency study, both the axial and radial velocity in a distance from the nozzle is shown in Fig. 1.

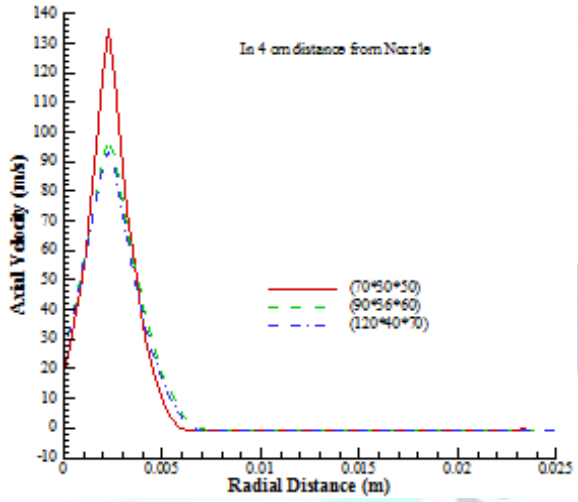


(a)

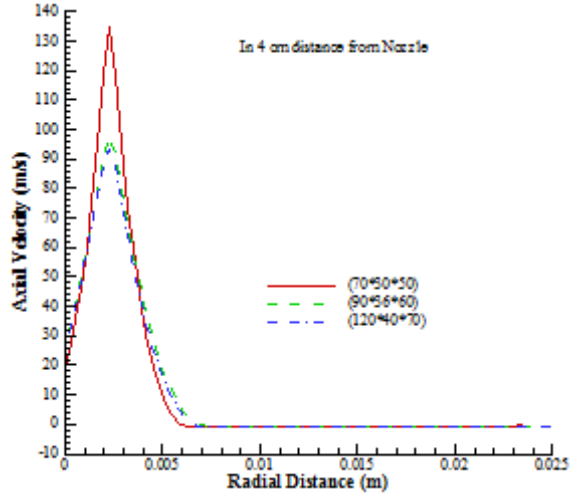


(b)

Fig. 1. Mesh independent results (a) axial velocity (b) radial velocity in 4 cm from nozzle

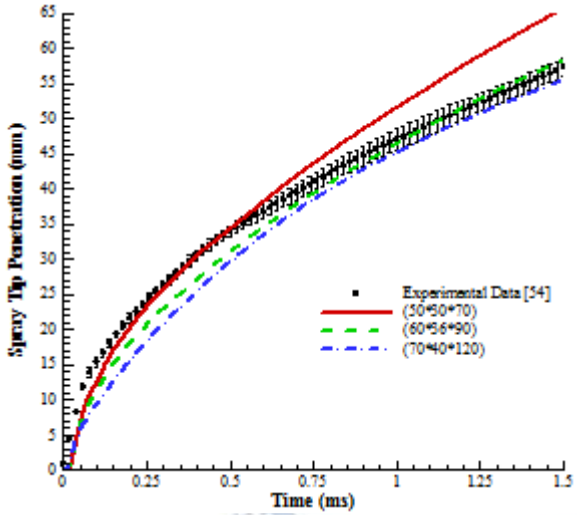


Fig. 2. Validated spray tip penetration results

## B. Validation

The experimental data set that is used for validating the computed results is for SANDIA experiments [17]. This set of data is the injection of n-Heptane fuel in a constant volume chamber. The conditions of this experiment were applied in an in-house CFD code. Details of the case chosen for comparison are summarized in Table II. Spray tip penetration results of three different computational meshes were compared to experimental data in order to choose grid independent results. The first grid has 105000 cells, the second grid has 194400 cells and the third one has 336000 cells (Fig. 2).

The results are promising when compared to experimental data and the second computational mesh has been chosen because of fewer computational efforts and at the same time having a high level of accuracy that shows in Fig. 1 and 2.

Table II.Transport equation variables

| Data Type | Quantity (Unit) | Data Type | Quantity (Unit) |
|---|---|---|---|
| Injection duration | 1.5 (ms) | Ambient temperature | 440 (K) |
| Fuel temperature | 363 (K) | Ambient pressure | 2.93 (MPa) |
| Injected mass | 3.46 (mg) | Ambient Nitrogen mole fraction | 100.0 (%) |
| Fuel type | n-Heptane | Nozzle diameter | 0.084 (mm) |

## C. Single parcel injection

This section presents the differences in choosing three different dispersion models on the behaviourof a single parcel which is injected in a constant volume chamber. In figures of this section, model of Gosman and Ionnadies [5] is declared as “simple random walk model”. First, the trajectory of a single parcel is studied under the same injection and chamber condition with different dispersion models (Fig. 3). This shows some differences in prediction of particle position between the random walk model and other models. But two more advanced modes predict somehow the same path for the particle.

Fig. 4 is the droplet evaporation history which shows a longer life time predicted by two more advanced dispersion models.

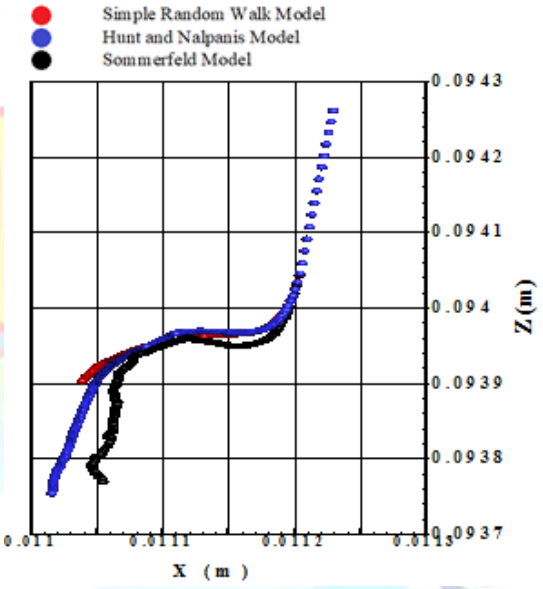


(a)

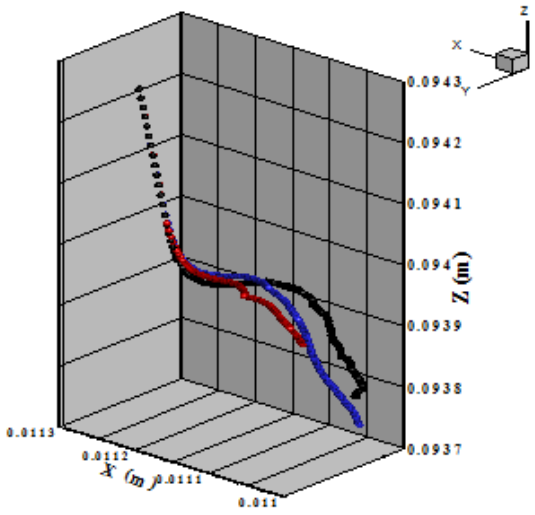


(b)

Fig. 3. Single parcel trajectory (a) Z-X plane (b) three-dimensional domain

Fig. 4 (a) shows twostages in droplet diameter versus time diagram. The first stage is an increase in droplet's diameter because of being in a hot environment which reduces the density. The second stage is a linear decrease in diameter which is also dictated by analytical solutions.

For assessing the performance of models in various chamber conditions, different initial turbulent kinetic energy has been chosen [18]. The initial value for turbulent kinetic energy in cells has been increased to show the change in models' performance in higher turbulence levels. It should be mentioned that the ratio of $(k_0/\varepsilon_0)$ is remained constant in all cases [19, 20]. It can be inferred from Fig. 5 that increasing the turbulence level of flow field does increase the penetration, but at the same time, it increases the evaporation rate. It is the reason that in some cases $(k_0 = 5\ KJ/Kg)$,the parcel travel fewer distances to evaporate completely.

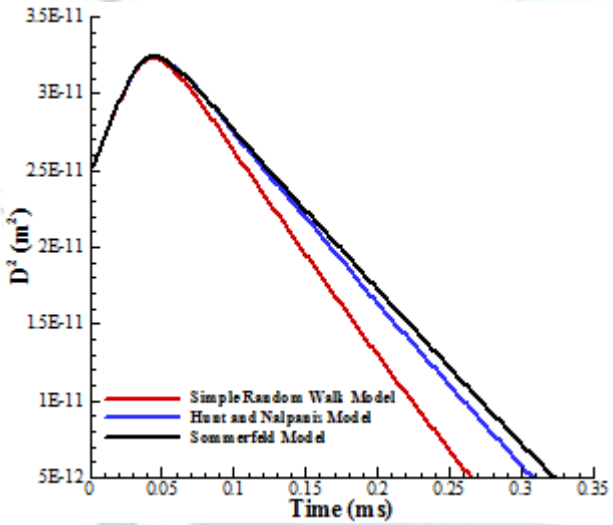


(a)

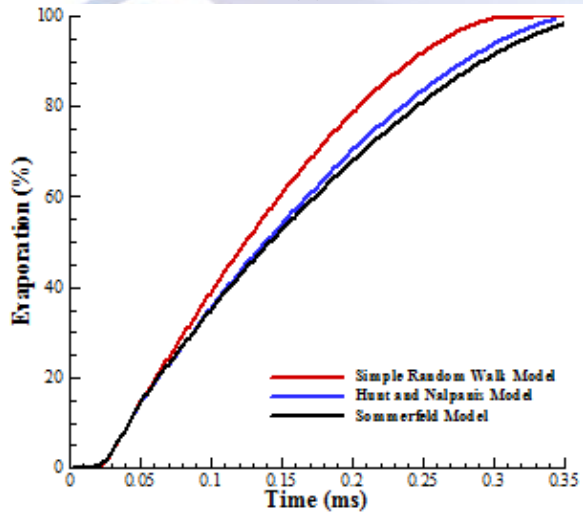


(b)

Fig. 4. (a) D2 vs. time (b) evaporation history by three different dispersion models

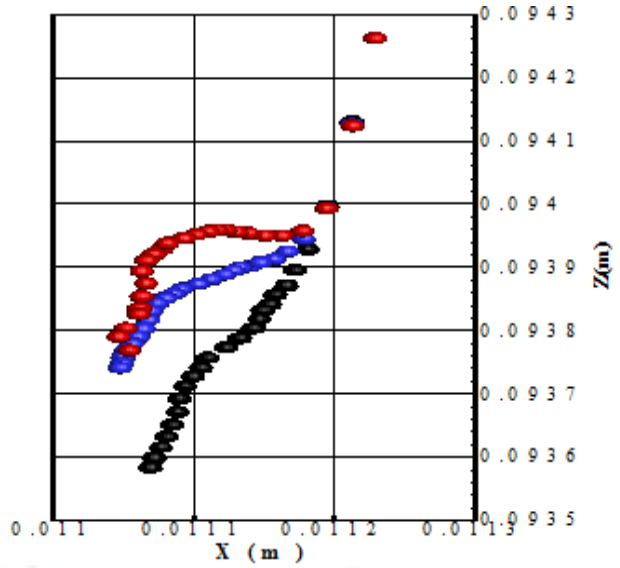


(a)

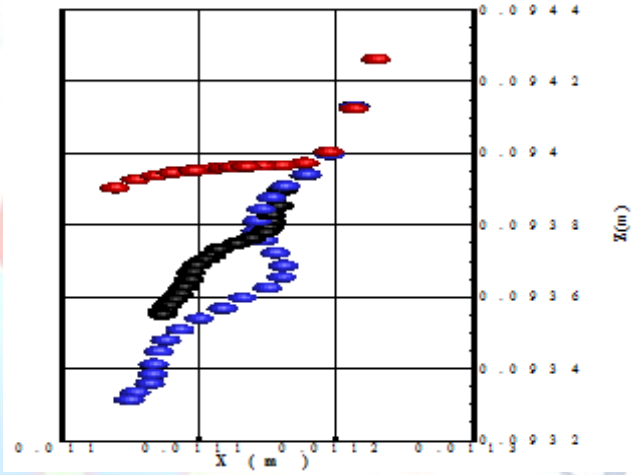


(b)

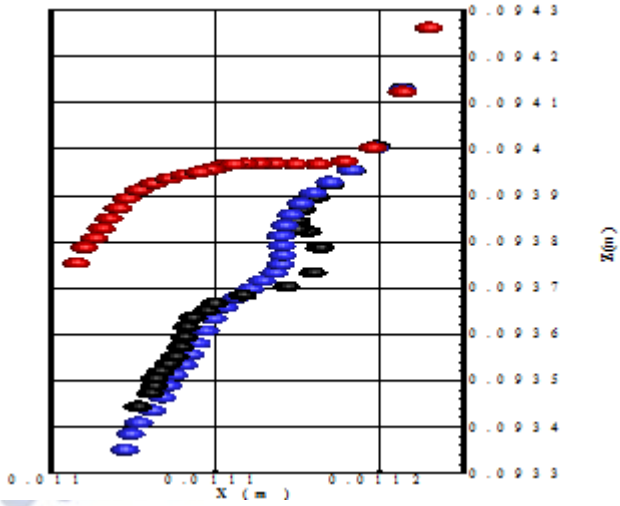


(c)

Fig. 5. (a) Simple random walk model (b) Hunt &Nalpanis model (c) Sommerfeld model Trajectory prediction with increasing initial turbulent kinetic energy.

### *D. Full spray injection*

By noticing differences in using differentdispersion models for single parcel

injection mode,it is conceivable that it should be an important factor in a complete spray of fuel.

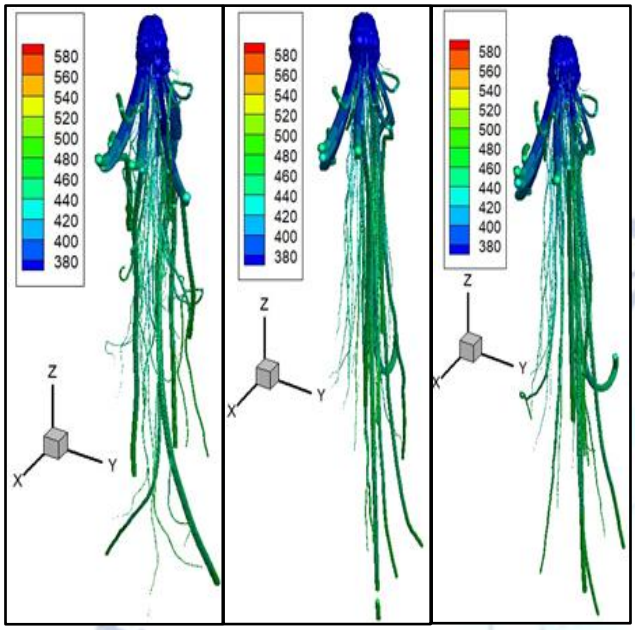


(a) (b) (c)

Fig. 6. (a) Simple random walk model (b) Hunt &Nalpanis model (c) Sommerfeld model Trajectory prediction in full spray mode

Fig. 6 is the pathways of a full spray injected vertically into the combustion chamber in injection duration. Fig. 6 shows that Sommerfeld model predicts a more dispersed structure of spray and fuel droplets travel more distances in the radial direction in comparison to two other models. But the spray tip penetration is predicted almost the same, using different models.

## IV. Conclusion

The main aim of this paper is to assess the potential of using different dispersion models for predicting droplet behavior in turbulent diesel engine sprays. First, the dispersion of a single parcel of droplets in a constant volume chamber was studied. It was found that using three different models chosen in this article, can lead to different behavior because of involving more parameters of the flow by more complex models to calculate the fluctuation velocity at the droplet position. It was shown that the Sommerfeld model predicts shorter droplet life time and the droplet traverse a longer path which can be a sign of higher fluctuation velocity. Next step was to find about the effect of different models in calculation of a complete diesel engine spray. It was shown that overall behavior is not affected drastically by choosing various models; but the Sommerfeld model (as it was the case for single parcel mode) predicts a more dispersed behaviour for full spray.

## References

[1] Cheng, Yung Sung, Aerosol deposition in the extrathoracic region, Aerosol Science & Technology, 37, (2003), 8, pp. 659-671.

[2] Tian, Lin, Goodarz, Ahmadi, Particle deposition in turbulent duct flows comparisons of different model predictions, Journal of Aerosol Science, 38, (2007), 4, pp. 377-397.

[3] Parker, Simon, Foat, Timothy, Preston, Steve, Towards quantitative prediction of aerosol deposition from turbulent flows, Journal of Aerosol Science, 39, (2008), 2, pp. 99-112.

[4] Yuu, Shinichi, Yasukouchi, Hirosawa, Jotaki, Particle turbulent diffusion in a dust laden round jet, AIChE Journal, 24, (1978), 3, pp. 509-519.

[5] Gosman, A, Ioannides, E, Aspects of computer simulation of liquid-fuelled combustors, AIAA 19th Aerospace Sciences Meeting paper AIAA-81-0323, St. Louis, USA, 1981.

[6] Berlemont, Alain, Grancher, M, Gouesbet, Gérard, Heat and mass transfer coupling between vaporizing droplets and turbulence using a Lagrangian approach, International journal of heat and mass transfer, 38, (1995), 16, pp. 3023-3034.

[7] Coimbra, C. F. M., J. S. Shirolkar, and M. Queiroz McQuay. "Modeling particle dispersion in a turbulent, multiphase mixing layer." Journal of Wind Engineering & Industrial Aerodynamics 73.1 (1998): 79-97.

[8] Hunt, J, Saltating and suspended particles over flat and sloping surfaces. I. Modelling concepts, Proc. Intl. Workshop on the Physics of Blown Sand, Department of Theoretical Statistics, Institute of Mathematics, University of Aarhus, 1985.

[9] Shahri PK, Shindgikar SC, HomChaudhuri B, Ghasemi A. Optimal Lane Management in Heterogeneous Traffic Network. InProceedings of the ASMA Dynamic Systems and Control Conference in Park City, Utah 2019.

[10] Taremi RS, Shahri PK, Kalareh AY. Design a Tracking Control Law for the Nonlinear Continuous Time Fuzzy Polynomial Systems. Journal of Soft Computing and Decision Support Systems. 2019 Nov 17;6(6):21-7.

[11] Lain, S., and M. Sommerfeld. "Turbulence modulation in dispersed two-phase flow laden with solids from a Lagrangian perspective." International Journal of Heat and Fluid Flow 24.4 (2003): 616-625.

[12] M. Sheikhshahrokhdehkordi, N. Goudarzi, F. Saffaraval, M. Mousavisani, P. Tkacik A TomoPIV flow field analysis of NACA 63-215 hydrofoil with CFD comparison. Proceedings of the Joint Fluid Engineering Conference, 2019, San Francisco, CA, US.

[13] M. Mousavisani, N. Goudarzi, M. Sheikhshahrokhdehkordi, T. Bisel, J. Dahlberg, P. Tkacik Exploring and improving the flow characteristics of an empty water channel test section: the application of TomoPIV and flowrate sensor for whole-flow-field visualization. Proceedings of the Joint Fluid Engineering Conference, 2019, San Francisco, CA, US.

[14] Borman, G,Johnson, John, Unsteady vaporization histories and trajectories of fuel drops injected into swirling air,SAE Technical Paper, No. 620271, 1962.

[15] Ranz, W. E., and W. R_ Marshall. "Evaporation from drops." Chem. eng. prog 48.3 (1952): 141-146.

[16] Reitz, Rolf, Diwakar, R, Effect of drop breakup on fuel sprays, SAE Technical Paper, . No. 860469, 1986.

[17] Sandia National Laboratories. Engine Combustion Network (ECN), Accessed 8 Nov, 2017; https//:ecn.sandia.gov/ecn-data-search/.
[18] H. Khaleghi, M. Ahmadi, H. Farani Sani. Effects of Two-Way Turbulence Interaction on the Evaporating Fuel Sprays, Journal of Applied Fluid Mechanics 12 (5), 1407-1415.
[19] H. Khaleghi, M. Ahmadi, H. Farani Sani. A comparative study of breakup models in diesel fuel spray, Iranian Society of Mechanical Engineering (ISME) 2017.
[20] Izadi V, Abedi M, Bolandi H. Novel FMECA Analysis Method in Attitude Control System. 11th Iran International Conference of Iranian Aerospace Society, 7, 2012.

International Journal for Modern Trends in Science and Technology
IJMTST